

## Building uniform and long-range ordered nanostructures on a surface by nucleation on a point defect array

This article has been downloaded from IOPscience. Please scroll down to see the full text article.

2006 J. Phys.: Condens. Matter 18 S17

(<http://iopscience.iop.org/0953-8984/18/13/S02>)

View [the table of contents for this issue](#), or go to the [journal homepage](#) for more

Download details:

IP Address: 129.252.86.83

The article was downloaded on 28/05/2010 at 09:14

Please note that [terms and conditions apply](#).

# Building uniform and long-range ordered nanostructures on a surface by nucleation on a point defect array

V Repain, S Rohart, Y Girard, A Tejada and S Rousset

Matériaux et Phénomènes Quantiques, UMR CNRS 7261, Université Paris 7, 2 place Jussieu  
75251 Paris Cedex, France

E-mail: [vincent.repain@paris7.jussieu.fr](mailto:vincent.repain@paris7.jussieu.fr)

Received 7 November 2005, in final form 4 January 2006

Published 13 March 2006

Online at [stacks.iop.org/JPhysCM/18/S17](http://stacks.iop.org/JPhysCM/18/S17)

## Abstract

We present both experimental and simulated results of ordered growth of cobalt nano-islands on a Au(111) vicinal template. Firstly, the temperature range for ordered growth and the islands size distributions are investigated by a rate equation model and kinetic Monte Carlo (KMC) simulations. Secondly, the incidence of the surface structure on the growth of cobalt is studied in detail by means of variable temperature scanning tunnelling microscopy experiments and KMC simulations. The underlying atomic processes responsible for the ordered growth are discussed.

## 1. Introduction

The fundamental research to determine the physical properties of nanostructures down to the atomic limit, as well as the practical applications, drives the need for the achievement of uniform nanostructure arrays. Since standard lithography techniques are intrinsically limited in resolution, new physical methods have to be used. The epitaxial growth has been shown to be an interesting alternative as either thermodynamic or kinetic processes can be involved to get uniform nanostructures on surfaces [1]. From a kinetic point of view, the self-assembly of nano-islands by nucleation on surfaces [2, 3] has proved to be a solution to randomly grow nanostructures with an adjustable size and density. However, the size distributions are always broad. The use of pre-structured templates provides an ordered growth regime under adequate flux and temperature conditions [4, 5]. In this case, nanostructures can be organized and size distributions are much narrower.

Metal on metal growth provides model systems for ordered growth on well defined nano-patterned substrates [4, 6, 7]. Experimentally, this phenomenon has been successfully applied to the formation of nanostructures but very few studies are dealing with the atomistic mechanisms leading to the organization and the quantitative determination of the associated energies. The

precise determination of the atomistic mechanisms for a given substrate should allow us to predict which material will display an ordered growth and the conditions (flux, temperature) for the narrowest size distribution.

In this paper, we study the ordered growth of Co islands on gold vicinal surfaces. Indeed, reconstructed Au(111) vicinal surfaces have been proved to be particularly good templates for ordered growth as they display a two-dimensional surface patterning coherent over macroscopic scales [8], which is usually not the case of patterned crystalline surfaces. In a first part, we present a simple kinetic model that gives some insights on ordered growth driven by a regular array of point defects (called traps in the following). Some analytical expressions are deduced for the temperature range where ordered growth is expected. The question of size distributions in such systems is also discussed by means of kinetic Monte Carlo (KMC) simulations. In a second part, we describe variable temperature scanning tunnelling microscopy (VT-STM) experiments of submonolayer Co growth on Au(788). A refined analysis of the experimental data is then proposed by means of comparison with KMC simulations. This allows us to evidence an interplay between an adsorption and a place exchange mechanism to explain the ordered growth between 65 and 300 K.

## 2. Theoretical insight for the nucleation on an atomic trap array

### 2.1. Island density scaling with temperature

Nucleation and growth of islands on surfaces has been extensively studied for many years and is reviewed in articles or books [9, 10]. The island density scaling with temperature has been shown to be a very important measurement since it gives access to the main parameters governing the nucleation and growth. The rate equation (RE) model for nucleation on homogeneous surfaces describes the time variation of the density of adatoms ( $n_1$ ) and stable islands ( $n_x$ ) [9]. We consider here that the binding energy between two adatoms is infinite i.e. dimers are stable. The main parameters of this model are the diffusion energy barrier  $E_d$ , the diffusion coefficient  $D_0$  and the adatom flux  $F$ . This model considers no deposition of adatoms onto an island, which means that it describes correctly only the low coverage regime. Moreover, it is important to point out that it is generally solved using a mean field approach of the nucleation and growth problem. To include the presence of traps on the surface we include two new parameters [11]:  $n_t$  the density of traps and  $E_t$  the trapping energy gain. This represents a preferred adsorption mechanism. We implement the homogeneous growth model by a set of equations for the time variation of trapped adatoms ( $n_{1t}$ ) and trapped stable islands ( $n_{xt}$ ).

The rate equations for  $n_1$ ,  $n_{1t}$ ,  $n_x$  and  $n_{xt}$  are the following:

$$\begin{aligned}
 \frac{dn_1}{dt} &= F - \sigma_1 D n_1 (2n_1 + n_{te} + n_{1t}) - \sigma_x D n_1 (n_x + n_{xt}) + n_{1t} v_0 e^{-(E_t + E_d)/k_B T} \\
 \frac{dn_{1t}}{dt} &= \sigma_1 D n_1 (n_{te} - n_{1t}) - n_{1t} v_0 e^{-(E_t + E_d)/k_B T} \\
 \frac{dn_x}{dt} &= \sigma_1 D n_1^2 \\
 \frac{dn_{xt}}{dt} &= \sigma_1 D n_1 n_{1t}
 \end{aligned} \tag{1}$$

$n_{te}$  is the empty trap density. Capture cross-sections of an adatom ( $\sigma_1$ ) and a stable island ( $\sigma_x$ ) are respectively taken as 3 and 7, since this is known to give a good description for low coverages [9, 12].

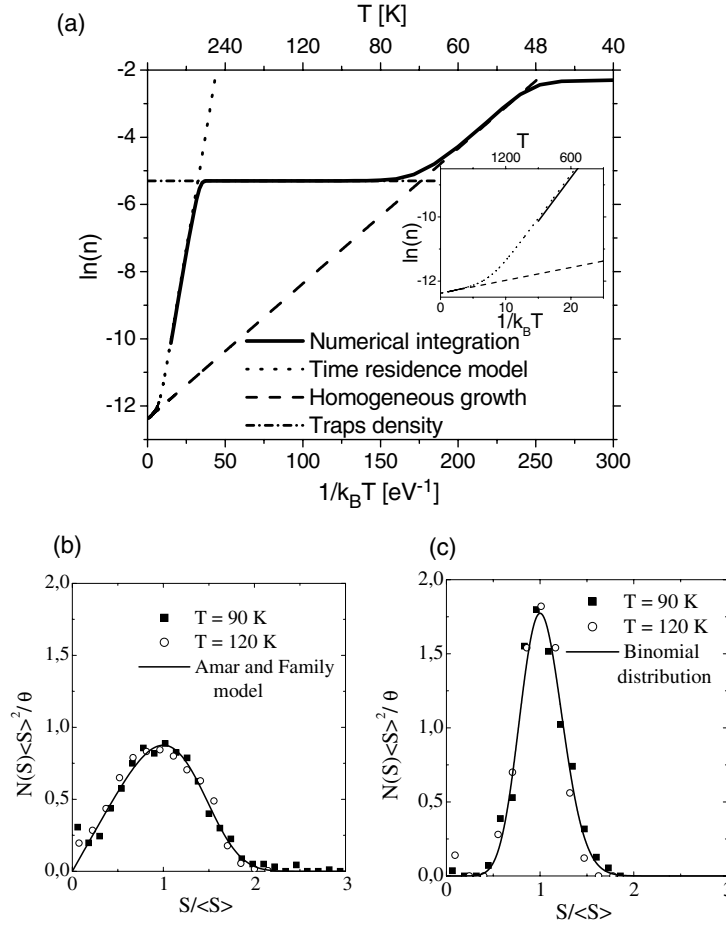


**Figure 1.** (a) Arrhenius plot of the island density (in islands/atomic sites) versus temperature calculated by numerical integration of equation (1). The analytical asymptotic regimes are also plotted (cf text). The inset shows a zoom of the high temperature regime. (b) Size distributions calculated by KMC for the growth on a homogeneous substrate at 90 and 120 K ( $\theta = 0.1$  ML). The full line shows the Amar and Family model. (c) Size distributions calculated by KMC for the growth on a heterogeneous substrate with a periodic array of atomic traps at 90 and 120 K ( $\theta = 0.1$  ML). The full line shows the binomial distribution associated with the Voronoï area of the traps lattice.

In order to describe the temperature behaviour of the nucleation process, we perform a numerical integration of equation (1) with the following parameters [13]:  $\nu_0 = 1/\tau_0 = 3.28 \times 10^{-12}$  Hz,  $D_0 = 8 \times 10^{11}$  sites  $s^{-1}$ ,  $E_d = 0.12$  eV,  $E_t = 0.7$  eV,  $n_t = 1/200$  atomic sites and  $F = 3.3 \times 10^{-3}$  ML  $s^{-1}$ . Integrating until the coverage  $\theta = 0.1$  monolayer (ML) gives the result in figure 1, which shows the Arrhenius plot of the island density versus the temperature.

Four different growth regimes are found according to the temperature. For low temperatures (below 45 K) no variation is found: the island density is constant with temperature. This corresponds to a low diffusion regime called ‘post-nucleation’ [9] when adatoms hardly diffuse on the surface and are stable. Between 45 and 70 K, a linear decrease of the logarithm of the island density with temperature is found. In this temperature range,

the island density is always higher than the trap density, which means that the adatom mean free path is shorter than the distance between traps. Therefore, there is no influence of the traps; the density variation with temperature is perfectly reproduced by the RE model result for homogeneous surfaces [9, 12], as shown in figure 1:

$$n = \eta(D_0/F)^{-1/3} \exp(E_d/3k_B T). \quad (2)$$

The prefactor  $\eta$  is calculated by integrating the RE equation for homogeneous growth. This leads to  $\eta = 0.07$  [9] and enables us to define the temperature  $T_o$  above which traps influence the nucleation. At this temperature, the density given by equation (2) equals the trap density  $n_t$ :

$$T_o = \frac{E_d}{k_B \ln \left[ \frac{D_0}{F} \left( \frac{n_t}{\eta} \right)^3 \right]}. \quad (3)$$

In the next temperature regime, lying from 70 to 300 K, the island density on the surface is constant and equals the trap density. This indicates that the nucleation is strongly governed by the traps on the surface. We call this regime ‘ordered growth’. The growth scenario is simple. In the early stage of growth, adatoms mainly reach the traps (nucleation regime). When all traps are occupied, additional adatoms mainly attach to existing islands without formation of islands out of trap positions. Using numerical integration we have calculated that the ratio of untrapped islands over the total number of islands is less than  $10^{-4}$  at 120 K. This regime ceases to operate when a trapped atom is no longer stable, i.e. the atom thermal energy is sufficient to allow atoms to jump out of the trap before another adatom is attached to it.

The last temperature regime displays a strong decrease of the island density with temperature. The characteristic of this regime is that trapping energy gain is no longer sufficient to stabilize atoms. Then, the influence of the traps becomes less important as the temperature increases. Considering the average adatom residence time in normal sites and traps, i.e.  $\langle t \rangle = (1 - n_t)\tau_0 e^{E_d/k_B T} + n_t\tau_0 e^{(E_d+E_t)/k_B T}$ , the linear decrease of the island density logarithm with temperature may be compared to a homogeneous growth model with an effective diffusion energy given by  $E_d^{\text{eff}}(T) = k_B T \ln(\langle t \rangle / \tau_0) = E_d + k_B T \ln[1 + n_t(e^{E_t/k_B T} - 1)]$  [13]. Combining the expression of the effective diffusion energy with equation (2), we plot the temperature behaviour of the island density in figure 1. This ‘time residence’ model [13] fits very well the numerical integration result. This illustrates the important role of traps for the diffusion and nucleation process. Indeed, even at high temperature, when the ordered growth regime is not observed anymore, traps still influence diffusion, which is driven by the time that adatoms spend in the traps. The real homogeneous growth regime without any influence of the traps is only recovered at very high temperature, over 2400 K (see the inset in figure 1). Using this model we can also estimate  $T_e$ , which is the highest temperature where organization is observed. Assuming that  $k_B T_e \ll E_t$ , we obtain

$$T_e = \frac{E_d + E_t}{k_B \ln \left[ \frac{D_0}{F} \frac{n_t^2}{\eta^3} \right]}. \quad (4)$$

## 2.2. Island size distributions

We now focus on the other key point of ordered growth, which is the achievement of narrow size distributions. Unfortunately, the mean field approach of the previous RE model cannot give any idea about the island size fluctuations during the nucleation and growth processes. Although a phenomenological model has been proposed for homogeneous growth by Amar and Family [14], very little is known for the growth on heterogeneous substrates, especially for ordered growth. In order to obtain some information on these size distributions, we have

performed some KMC simulations (the details on the algorithm can be found in [15]) with the same parameters as used for the integration of the RE model. Some results of these simulations are shown in figures 1(b) and (c), which are the case of a homogeneous surface and a surface prestructured with a rectangular array of traps respectively. The homogeneous growth size distributions are perfectly reproduced by the Amar and Family model [14] and show typical full widths at half maximum (FWHM) of 110%, whatever the temperature. In the case of the growth on the prestructured surface, when nucleation occurs on the traps ( $T_o < T < T_e$ ), the size distributions are narrower and are almost constant with temperature in this range. The FWHM for  $n_t = 1/200$  and  $\theta = 0.1$  MC is typically 50%. Interestingly, these size distributions are very well fitted by simple binomial distributions  $p(k) = C_k^n \theta^k (1 - \theta)^{n-k}$  with  $k$  the island size (in number of atoms) and  $n$  the number of atomic sites of the Voronoï area in the trap lattice (i.e.  $n = 1/n_t$ ). This fact had already been pointed out for the ordered growth of Ag/Ag(2 ML)/Pt(111) [4] but is less trivial for growth induced by point defect nucleation. This means that during the growth regime the probability that an adatom deposited on the surface does not stick to its closest island is vanishingly small, whatever the coverage or the temperature between  $T_o$  and  $T_e$ , at least with parameters in our simulations. Moreover, simulations on randomly distributed atomic traps show a broadening of the island size distribution due to the distribution of trap Voronoï areas. This confirms that the analysis of size distributions in terms of the Voronoï area distribution is always pertinent. Therefore, the FWHM of the size distribution is limited to the perfectness of the trap array for a given coverage. In addition, even for a perfect trap array, there is an intrinsic statistical limit to the size distribution width. As for the binomial distribution the variance is  $\sigma = \sqrt{(1 - \theta)/n\theta}$ , the only way to improve the size distribution quality is to increase the coverage and/or use a surface with a lower trap density (larger Voronoï cells).

### 3. Two-dimensional long-range ordered growth of Co islands on a Au(111) vicinal template

#### 3.1. Experimental results

We now describe the experimental results of the submonolayer growth of Co on Au(788) in the 35–480 K temperature range. The Au(788) surface is a vicinal surface of Au(111) which displays a highly periodic step edge array combined with a surface reconstruction similar to the  $22 \times \sqrt{3}$  reconstruction of Au(111). The surface unit cell has the following dimensions: 3.9 nm along the  $[\bar{2}11]$  direction and 7.2 nm along the  $[01\bar{1}]$  direction. This surface has already been described in detail elsewhere [16], as well as the surface preparation, the deposition and the imaging procedures [15]. It is worthwhile to note that the growth morphology seems to be essentially controlled by kinetic parameters. Indeed, after the Co deposition at low temperature, a heating cycle of the substrate gives rise to a partial coalescence of small islands. In contrast, a cooling cycle has no influence on the island morphology, which excludes some strain induced thermodynamic morphological transitions as the driving force for the ordered growth regime [1]. Therefore, in the following, the experimental data will be analysed as the result of kinetic processes. We observe an ordered growth of Co on this substrate in a temperature range from 65 to 300 K. Figure 2 shows typical STM images for different temperatures from 35 to 480 K. The low temperature regime (cf figure 2(a)) is very similar to what would be expected on a homogeneous substrate. The islands are randomly distributed and the size distribution is well fitted by an exponential decay, which is typical of a post-nucleation regime [9]. Above 65 K, most of the islands are located at very precise locations on the surface. STM images at very low coverage have shown that the favoured nucleation sites are located at

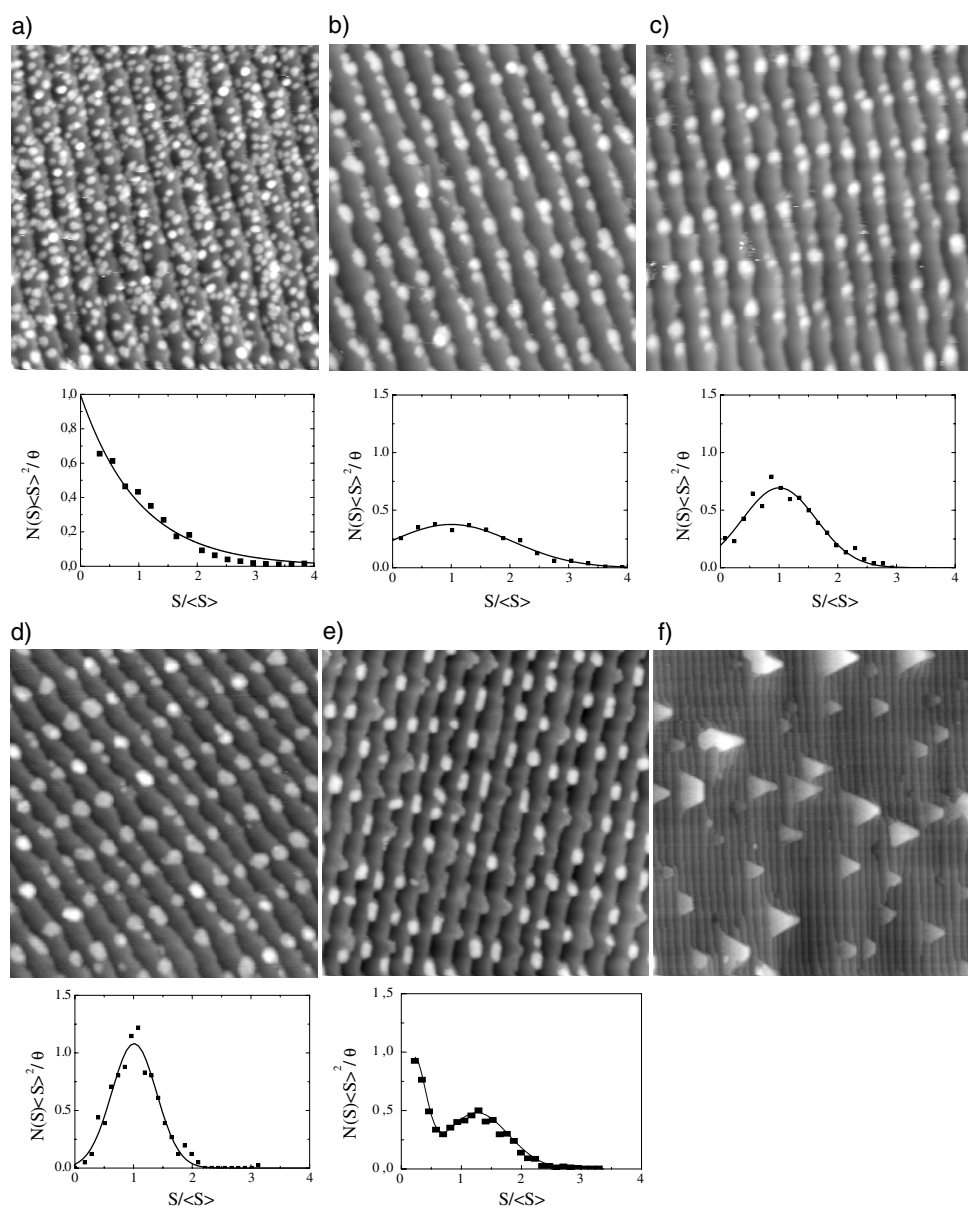


**Figure 2.** STM images of submonolayer Co deposited on Au(788) for various temperatures and their corresponding normalized Co island size distribution. Full lines are either exponential decay or Gaussian functions which fit the distribution. (a)  $50 \times 50 \text{ nm}^2$ ,  $T = 40 \text{ K}$ ,  $\theta = 0.6 \text{ ML}$ . (b)  $50 \times 50 \text{ nm}^2$ ,  $T = 95 \text{ K}$ ,  $\theta = 0.4 \text{ ML}$ . (c)  $60 \times 60 \text{ nm}^2$ ,  $T = 135 \text{ K}$ ,  $\theta = 0.3 \text{ ML}$ . (d)  $60 \times 60 \text{ nm}^2$ ,  $T = 170 \text{ K}$ ,  $\theta = 0.3 \text{ ML}$ . (e)  $60 \times 60 \text{ nm}^2$ ,  $T = 300 \text{ K}$ ,  $\theta = 0.2 \text{ ML}$ . (f)  $150 \times 150 \text{ nm}^2$ ,  $T = 480 \text{ K}$ ,  $\theta = 0.6 \text{ ML}$ .

one or two atomic rows from the step edges and at the edge of discommensuration lines [15]. At higher coverage, this leads to a doublet of islands per surface unit cell. It can happen that these two islands coalesce and form a bigger single island. The growth morphology does not change significantly between 65 and 200 K. However, there is a narrowing of the size distribution with



increasing temperature, essentially due to the fact that alignment of small islands along the step edges disappears (cf figures 2(b) and (d)). Above 200 K islands are still organized but grow on both sides of the step edges. Moreover, their growth is more anisotropic, leading to a rectangular shape. Around 300 K, within a 20 K temperature range, the growth ceases to be ordered. At 300 K, although every island is located around a favoured nucleation site, we observe a large inhomogeneity in the filling of favoured sites and in the island size. This leads to multimodal size distributions, depending on the coverage, with typically a large number of small islands together with larger ones (cf figure 2(e)). Above 300 K, the island density decreases with temperature and less correlation is observed between islands. Moreover, above 400 K, the islands are several atomic layers high and the island shape changes to a truncated triangle, certainly related to the equilibrium shape of such Co islands (cf figure 2(f)).

From these STM images at different temperatures, we can extract some data by a statistical analysis. As outlined in the previously described RE model, a very pertinent quantity in the nucleation and growth process is the island density. For each temperature, we have performed many experiments at different coverages and measured the island density as a function of coverage. The maximum of this density is called the critical density and is generally related to the mean diffusion length of Co adatoms on the surface. The experimental plot of this quantity as a function of temperature, in an Arrhenius representation, is shown in figure 3. The shape of this curve is very close to what has been deduced previously from the RE model. The low temperature regime shows a post-nucleation regime followed by a homogeneous-like diffusion regime. A large plateau associated with the ordered growth regime spreads from 65 to 300 K. Above 300 K, we recover a diffusion regime with a strong decrease of the island density with temperature. From the measured temperature range for the ordered growth and equations (3) and (4) we can deduce an estimate of  $E_d = 0.12$  eV and  $E_t = 0.7$  eV. We note that the diffusion energy is in good agreement with previous quenched molecular dynamics (QMD) calculations [17]. In the following, we will discuss the trapping energy value.

### 3.2. Trapping mechanism

We now focus on the trapping energy mechanism in order to understand the high  $E_t$  value. This value is intriguing. Indeed, a preferred adsorption mechanism can hardly show such a deep potential for a metal on metal system. For example, QMD calculations for Co/Au(111) estimate  $E_t = 0.1$  eV on top of the discommensuration lines [18]. The value found in the case of Co/Au(788) should reflect a more complex mechanism. Following experimental STM observations at room temperature [8], we have considered a preferred place exchange mechanism. The trapping mechanism now involves a combination of two mechanisms: first the adatom is trapped due to the preferred adsorption mechanism, and subsequently it can exchange with the underneath gold surface atom. These two mechanisms imply a set of three energetic parameters: the energy gain for the preferred adsorption mechanism  $E_{t,ads}$ , the energy gain when the Co adatom is inserted into the gold surface layer  $E_{t,ex}$  and the place exchange energy barrier  $\Delta E_{ex}$  (cf scheme of figure 3(a)). This last parameter was estimated to be about 0.3 eV [15]. The lattice of atomic traps has been deduced from atomically resolved STM images at very low coverage. In the [011] direction, two traps separated by seven atomic sites are periodically reproduced every 25 atomic sites. In the  $[\bar{2}11]$  direction, the period is 16 atomic rows. This leads to a trap density  $n_t = 1/200$ .

Using KMC simulations, a good fit of the experimental data is achieved with the combination of both mechanisms in the preferred sites (see figure 3(a)) [15]. For this simulation we have  $\Delta E_{ex} = 0.32$  eV, which ensures that no place exchange occurs before 200 K. The energy to leave the preferred sites (removal process for the place exchange) is  $E_{rem} = 0.82$  eV ( $E_{t,ex} + \Delta E_{ex} - E_{t,ads}$ ). This value corresponds to the sum of  $E_t$  and  $E_d$  used in the RE model.



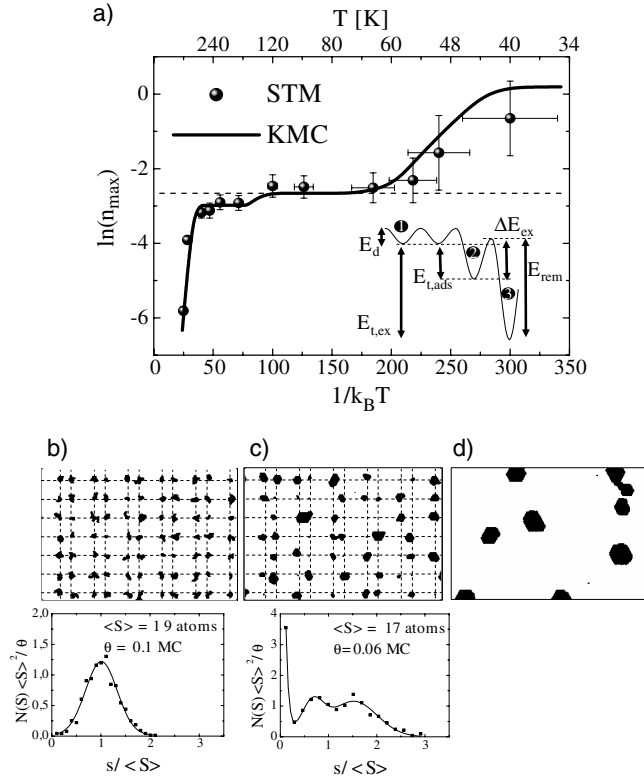


**Figure 3.** (a) Experimental data and KMC simulation of the critical island density  $n_c$  (in islands  $\text{nm}^{-2}$ ) versus the temperature for the growth of Co on Au(788). A good fit of the experimental data for the critical island density versus the temperature is obtained with a model combining both the adsorption and place exchange mechanisms in the preferred sites. Inset: energetic scheme of the trapping mechanism. The numbers refer to (1) a normal site, (2) a preferred adsorption, and (3) a place-exchanged atom. (b)–(d) KMC images and their corresponding size distributions. (b)  $20 \times 40 \text{ nm}^2$ ,  $T = 80 \text{ K}$ ,  $\theta = 0.1 \text{ ML}$ . (c)  $20 \times 40 \text{ nm}^2$ ,  $T = 300 \text{ K}$ ,  $\theta = 0.06 \text{ ML}$ . (d)  $50 \times 75 \text{ nm}^2$ ,  $T = 500 \text{ K}$ ,  $\theta = 0.05 \text{ ML}$ .

These KMC parameters can be compared with those obtained by QMD and a global good agreement is found [15].

In figure 3, a plateau with exactly one dot per preferred site is found in the 65–150 K temperature range. Only the preferred adsorption mechanism is able to explain this plateau. Indeed, at such a low temperature, the exchange energy barrier prevents the exchange from being observed [15]. It should be pointed out that the KMC images shown in figure 3 are in good agreement with STM experiments. This definitely confirms that the best condition for a long range ordered growth with a narrow island size distribution is a sample deposition temperature around 130–150 K. Above 150 K, the adsorption energy gain is not sufficient anymore in order to stabilize the adatoms. However, the organization is kept due to the activation of the place exchange mechanism. Then a rough organization is maintained up to 300 K, i.e., the number of islands per preferred site is between 1 and 2. The most important point, in this temperature range, is that the order still exists on the surface (see figure 2(e)). However, the number of defects (empty favoured site, coalesced neighbouring dots, . . .) is more important than in the previous regime. This result is particularly clearly seen at  $T = 300 \text{ K}$ . At

this temperature, the experimental bimodal size distribution is pretty well reproduced, as shown by figure 3(c). The origin of these inhomogeneities is the weakness of the bonds between the Co atoms: at 300 K, the critical size (largest unstable island) of an island in a preferred site is 2. This explains why the growth of the dots in the preferred sites is strongly inhomogeneous: some dots grow faster and lead to large islands when they coalesce with the neighbouring islands.

The end of the plateau is much better reproduced by KMC than by RE calculation. This is also due to the influence of the dimer bonds: in RE calculation the possibility for a dimer to break is neglected although the dimer binding energy (0.52 eV) is small with respect to the temperatures at the end of the plateau (about  $T = 300$  K).

The originality of the growth of Co on Au(788) is the two-state trapping mechanism, which enables us to observe ordered growth in a wide temperature range. An important point for this is the interplay between both adsorption and place exchange mechanisms. This is a key point in order to maintain the organization on such a wide temperature span. The interplay only occurs if the removal process energy of the adsorption ( $E_d + E_{t,ads}$ ) is higher than the place exchange barrier  $\Delta E_{ex}$ . In the case of Co on Au(788) these energies are very close. This explains why the interplay is not perfect and leads to a small accident around 150 K in the curve of the critical island density versus temperature (see figure 3(a)).

#### 4. Conclusion

The ordered growth of Co nanodots on the Au(788) surface is proven to be due to the presence of preferred sites. The origin of the preferred sites together with the atomic process responsible for the organization is clearly elucidated. The ordered growth regime occurs on a wide temperature range [ $T_o$ ,  $T_e$ ]. In the framework of the RE model,  $T_o$  and  $T_e$  are respectively determined by two key energy parameters  $E_d$ , the diffusion energy and  $E_t$ , the energy to leave the preferred sites. For temperatures below  $T_o$ , organization is limited by the adatom diffusion length. Above  $T_e$ , the energy gain in the preferred sites is no longer sufficient to stabilize the adatoms and to lead to an ordered array of islands. The particularity of the ordered growth of Co on Au(788) is that it occurs for a very large temperature range (65, 300 K). This is explained by a mechanism which combines a strong energy gain with a low activation barrier. In this case, we have identified each mechanism. We found that this can be achieved by an interplay between two mechanisms: adsorption (low activation barrier) and place exchange (high energy gain). The calculations show that the interplay is efficient when the energy gain of the adsorption is higher than the activation energy of the place exchange. Further experiments and calculations for deposition of other materials on other reconstructed surfaces should be of interest to confirm our nucleation and growth scenario. The influence of different thermodynamic parameters such as the lattice mismatch or electronic surface state confinement on the ordering and their interplay with kinetic processes would also be of great interest to get a deeper insight into the metastability of these ordered systems.

#### Acknowledgments

We thank H Bulou and C Goyhenex for the QMD calculations and L Proville for his help with the KMC simulations.

#### References

- [1] Shchukin V A, Ledentsov N N and Bimberg D 2003 *Epitaxy of Nanostructures* (Berlin: Springer)
- [2] Röder H, Hahn E, Brune H, Bucher J-P and Kern K 1993 *Nature* **366** 141

- 
- [3] Teichert C 2002 *Phys. Rep.* **365** 335
  - [4] Brune H, Giovannini M, Bromann K and Kern K 1998 *Nature* **394** 451
  - [5] Leroy F, Eymery J, Gentile P and Fournel F 2002 *Appl. Phys. Lett.* **80** 3078
  - [6] Chambliss D, Wilson R and Chiang S 1991 *Phys. Rev. Lett.* **66** 1721
  - [7] Ellmer H, Repain V, Sotto M and Rousset S 2002 *Surf. Sci.* **511** 183
  - [8] Repain V, Baudot G, Ellmer H and Rousset S 2002 *Europhys. Lett.* **58** 730
  - [9] Brune H 1998 *Surf. Sci. Rep.* **31** 121
  - [10] Venables J 2000 *Introduction to Surface and Thin Film Processes* (Cambridge: Cambridge University Press)
  - [11] Venables J 1997 *Physica A* **239** 35
  - [12] Venables J 1972 *Phil. Mag.* **17** 697
  - [13] Rohart S, Baudot G, Repain V, Girard Y and Rousset S 2005 *J. Cryst. Growth* **275** e203
  - [14] Amar J G and Family F 1995 *Phys. Rev. Lett.* **74** 2066
  - [15] Rohart S, Baudot G, Repain V, Girard Y, Rousset S, Bulou H, Goyhenex C and Proville L 2004 *Surf. Sci.* **559** 47
  - [16] Rousset S, Repain V, Baudot G, Garreau Y and Lecoeur J 2003 *J. Phys.: Condens. Matter* **15** S3363
  - [17] Bulou H and Goyhenex C 2002 *Phys. Rev. B* **65** 45407
  - [18] Goyhenex C and Bulou H 2001 *Phys. Rev. B* **63** 235404